

Criticality and Inflation of the Gauged B-L Model

Kiyoharu Kawana*

Department of Physics, Kyoto University, Kyoto 606-8502, Japan

December 3, 2024

Abstract

We consider the multiple point principle (MPP) and the inflation of the gauged B-L extension of the Standard Model (SM) with a classical conformality. We examine whether the scalar couplings and their beta functions can become simultaneously zero at $\Lambda_{\text{MPP}} := 10^{17}$ GeV by using the two-loop renormalization group equations (RGEs). We find that we can actually realize such situation and that the parameters of the model are uniquely determined by the MPP. However, as discussed in [26], if we want to realize the electroweak symmetry breaking by the radiative B-L symmetry breaking, the self coupling λ_Ψ of a newly introduced SM singlet complex scalar Ψ must have a non-zero value at Λ_{MPP} , which means the breaking of the MPP. We find that the $\mathcal{O}(100)$ GeV electroweak symmetry breaking can be achieved even if this breaking is very small; $\lambda_\Psi(\Lambda_{\text{MPP}}) \leq 10^{-10}$. Within this situation, the mass of the B-L gauge boson is predicted to be

$$M_{B-L} = 3.4 \times \sqrt{\frac{\lambda(v_h)}{0.10}} \times v_h \simeq 836 \text{ GeV},$$

where λ is the Higgs self coupling and v_h is the Higgs expectation value. This is a remarkable prediction of the (slightly broken) MPP. Furthermore, such a small λ_Ψ opens a new possibility: Ψ plays a roll of the inflaton [28]. The another purpose of this paper is to investigate the $\lambda_\Psi \Psi^4$ inflation scenario with the non-minimal gravitational coupling $\xi \Psi^2 \mathcal{R}$ based on the two-loop RGEs.

*E-mail: kiyokawa@gauge.scphys.kyoto-u.ac.jp

1 Introduction

The discovery of the Higgs like particle and its mass [1, 2] is very meaningful for the Standard Model (SM). The experimental value of the Higgs mass suggests that the Higgs potential can be stable up to the Planck scale M_{pl} and also that both of the Higgs self coupling λ and its beta function β_λ become very small around M_{pl} . This fact attracts much attention, and there are many works which try to find its physical meaning [3, 4, 5, 6, 7, 8, 9, 10, 11, 12, 13, 14, 15, 16, 17, 18, 19, 20, 21, 22].

Well before the discovery of the Higgs, it was argued that the Higgs mass can be predicted to be around 130GeV by the requirement that the Higgs potential becomes flat at M_{pl} [3, 4]. Such a requirement (not always at M_{pl}) is generally called the multiple point principle (MPP). One of the good points of the MPP is its predictability to the parameters of a low energy effective theory. For example, the values of the scalar couplings are radiatively generated by the renormalization group equations (RGEs), and the flatness of the potentials furthermore gives the strong relations between parameters. As a result, the low-energy effective couplings can be uniquely predicted by the MPP. See [23, 24] for example.

By taking the fact that the MPP can be realized in the SM into consideration, a natural question is whether such a criticality can be also realized in the models beyond the SM. One of the interesting extensions is the gauged B-L model with a classical conformality [25, 26, 27, 28]. Here, “classical conformality” means there is no mass term at the classical level without gravity. This model can be obtained by gauging the global $U(1)_{B-L}$ symmetry of the SM with the three right-handed neutrinos and a SM singlet complex scalar Ψ . As discussed in the following, if we neglect the Yukawa couplings between the Higgs and neutrinos, there are six unknown parameters in this model. Especially, two of them are new scalar couplings: κ and λ_Ψ . Therefore, in principle, these six parameters can be uniquely fixed by the MPP conditions:

$$\lambda(\Lambda_{\text{MPP}}) = \lambda_\Psi(\Lambda_{\text{MPP}}) = \kappa(\Lambda_{\text{MPP}}) = \beta_\lambda(\Lambda_{\text{MPP}}) = \beta_{\lambda_\Psi}(\Lambda_{\text{MPP}}) = \beta_\kappa(\Lambda_{\text{MPP}}) = 0, \quad (1)$$

where Λ_{MPP} is the scale at which we impose the MPP. The analyses in this paper are based on the following assumptions:

1. We consider the MPP at $\Lambda_{\text{MPP}} = 10^{17}$ GeV.
2. As well as the analyses in [25, 26], we do not include mass terms in the Lagrangian. As a result, all the low energy scales are radiatively generated.
3. The Higgs mass is fixed at

$$M_h = 125.7\text{GeV}, \quad (2)$$

and we regard the top mass M_t as one of the free parameters.

4. We assume that the small neutrino masses are produced by the seesaw mechanism via the radiative breaking of the B-L symmetry. As a result, we can neglect the Yukawa couplings y_ν between the Higgs and the neutrinos because the typical breaking scale is very small ($\ll 10^{13}\text{GeV}$).

In subsection 2.2, we will see that Eq.(1) can be actually realized at $\Lambda_{\text{MPP}} = 10^{17}\text{GeV}$.

One of the good features of this model is that the electroweak symmetry breaking can be triggered by the $U(1)_{\text{B-L}}$ symmetry breaking via the Coleman-Weinberg (CW) mechanism. In [26], it was argued that we can naturally obtain $v_h = \mathcal{O}(100)\text{GeV}$ by imposing $\lambda(M_{pl}) = 0$ and $\kappa(M_{pl}) = 0$. Here, the important point is that $\lambda_\Psi(\Lambda_{\text{MPP}}) \neq 0$ is needed to realize such B-L breaking¹. Therefore, if we try to combine this fact and the MPP, a natural question arises:

- *Is the $\mathcal{O}(100)\text{GeV}$ electroweak symmetry breaking possible even if $\lambda_\Psi(\Lambda_{\text{MPP}})$ is small ?*

In subsection 2.3, we will see that this is actually possible even if $\lambda_\Psi(\Lambda_{\text{MPP}}) \leq 10^{-10}$. The reason is very simple: By tuning the parameters of the model, we can obtain the favorable scale at which $U(1)_{\text{B-L}}$ breaks so that v_h becomes $\mathcal{O}(100)\text{GeV}$. Therefore, the B-L model is a phenomenologically very interesting model in that it can explain the natural-scale electroweak symmetry breaking while satisfying the (slightly broken) MPP. Furthermore, within this situation, we find that the mass of the B-L gauge boson is predicted to be

$$M_{B-L} = 2g_{B-L}(v_{B-L})v_{B-L} = 2.3 \times \sqrt{\frac{\lambda(v_h)}{0.10}} \times v_h \simeq 836 \text{ GeV}, \quad (3)$$

where v_{B-L} is the expectation value of Ψ and we have used the typical value $\lambda(v_h) \simeq 0.1$. This is a remarkable prediction of the (slightly broken) MPP, and it is surprising that the predicted value of M_{B-L} depends only on the SM parameters².

On the other hand, there are many observational results from the cosmological side. One of the reliable possibilities to explain them is the cosmic inflation. As is well known, the Higgs inflation is possible in the SM where the criticality of the Higgs potential plays an important role to realize the inflation naturally [17]. Of course, such a Higgs inflation is possible in the B-L model, but, we can also consider the inflation scenario where Ψ plays a roll of the inflaton [28]. In this paper, we study the $\lambda_\Psi\Psi^4$ inflation with the non-minimal gravitational coupling $\xi\Psi^2\mathcal{R}$. Our analysis is based on the following condition:

¹Realizing the B-L symmetry breaking when $\lambda_\Psi(\Lambda_{\text{MPP}}) = 0$ is difficult. See Section2.

²Unfortunately, this value of M_{B-L} is already excluded by the experiment of ATLAS [29]. See subsection 2.3.

	$SU(3)_c$	$SU(2)_L$	$U(1)_Y$	$U(1)_{B-L}$
Q_L^i	3	2	+1/6	+1/3
u_R^i	3	1	+2/3	+1/3
d_R^i	3	1	-1/3	+1/3
ℓ_L^i	1	2	-1/2	-1
ν_R^i	1	1	0	-1
e_R^i	1	1	-1	-1
H	1	2	-1/2	0
Ψ	1	1	0	+2

Table 1: The particle contents of the B-L model and their charges except for the gauge bosons. Here, i represents the generation.

- *We consider the inflation under the situation where the Higgs potential is flat at $\Lambda_{MPP} = 10^{17} \text{ GeV}$ and the electroweak symmetry breaking occurs at $\mathcal{O}(100) \text{ GeV}$.*

In the following discussion, we will see that this condition strongly constrains the parameters, and as a result, we can obtain the unique cosmological predictions³ which are consistent with the recent observed values by Planck [32] and BICEP2 [33].

This paper is organized as follows. In Section 2, we study the MPP and the B-L symmetry breaking from the point of view of the slightly broken MPP. In Section 3, we investigate the inflation scenario where the SM singlet complex scalar Ψ plays a roll of the inflaton. In Section 4, we give summary.

2 MPP of the B-L Model and Symmetry Breaking

The flow of this section is as follows. In subsection 2.1, we shortly review the gauged B-L model. In subsection 2.2, we consider the MPP of this model. In subsection 2.3, we study whether the $\mathcal{O}(100) \text{ GeV}$ electroweak symmetry breaking can be realized even if λ_Ψ (Λ_{MPP}) is very small.

2.1 Short Review of the B-L Model

In this subsection, we shortly review the B-L extension of the SM. Here, our discussion is mainly based on [30]. As mentioned in the introduction, this model can be obtained by gauging the global $U(1)_{B-L}$ symmetry. The kinetic terms of the two $U(1)$ gauge

³Here, we use “unique” in the sense that our predictions do not so depend on the parameters of the model except for λ_Ψ , ξ and the initial value of Ψ .

fields are given as follows:

$$\mathcal{L}_{kin} = -\frac{1}{4}F^{\mu\nu}F_{\mu\nu} - \frac{1}{4}F_{B-L}^{\mu\nu}F_{B-L\mu\nu} - \frac{\omega}{4}F_{B-L}^{\mu\nu}F_{\mu\nu}, \quad (4)$$

where $\omega(\in \mathbb{R})$ represents the kinetic mixing. The U(1) part of the covariant derivative of a matter field ϕ_k is given by

$$\mathcal{D}_\mu = \partial_\mu + i \sum_{i=1}^2 \sum_{j=1}^2 Y_k^i g_{ij} A_\mu^j, \quad (5)$$

where A_μ^1 and A_μ^2 are the gauge fields of $U(1)_Y$ and $U(1)_{B-L}$ respectively, Y_k^i are the U(1) charges and g_{ij} represent the U(1) gauge couplings. We can remove the mixing term by changing A_μ^1 and A_μ^2 to the new fields A_μ^Y and A_μ^{B-L} :

$$A_\mu^1 = \frac{1}{\sqrt{2(1+\omega)}}A_\mu^Y + \frac{1}{\sqrt{2(1-2\omega)}}A_\mu^{B-L}, \quad A_\mu^2 = \frac{1}{\sqrt{2(1+\omega)}}A_\mu^Y - \frac{1}{\sqrt{2(1-2\omega)}}A_\mu^{B-L}. \quad (6)$$

We simply express Eq.(6) as $A_\mu^i = \sum_\alpha R_\alpha^i A_\mu^\alpha$. By this transformation, the new gauge couplings are

$$g'_{i\alpha} := \sum_j g_{ij} R_\alpha^j. \quad (7)$$

We denote $g'_{i\alpha}$ as g_{YY} , g_{YE} , g_{EY} and g_{EE} without a prime in the following discussion. Only three of them are meaningful because we can further rotate the gauge fields without producing the mixing term:

$$\begin{pmatrix} A^Y \\ A^{B-L} \end{pmatrix} = \begin{pmatrix} \cos \theta & -\sin \theta \\ \sin \theta & \cos \theta \end{pmatrix} \begin{pmatrix} \tilde{A}^Y \\ \tilde{A}^{B-L} \end{pmatrix}.$$

Thus, we can choose the angle θ so that one of $g_{\alpha\beta}$ vanishes. For convenience, we take the following bases:

$$B_\mu := \frac{g_{EE}A_\mu^{B-L} + g_{EY}A_\mu^Y}{\sqrt{g_{EE}^2 + g_{EY}^2}}, \quad E_\mu := \frac{-g_{EY}A_\mu^{B-L} + g_{EE}A_\mu^Y}{\sqrt{g_{EE}^2 + g_{EY}^2}}. \quad (8)$$

In this bases, the second term of Eq.(5) becomes

$$g_Y Y_k^Y B_\mu + (g_{B-L} Y_k^{B-L} + g_{\text{mix}} Y_k^Y) E_\mu, \quad (9)$$

where

$$g_Y := \frac{g_{EE}g_{YY} - g_{EY}g_{YE}}{\sqrt{g_{EE}^2 + g_{EY}^2}}, \quad g_{B-L} := \sqrt{g_{EE}^2 + g_{EY}^2}, \quad g_{\text{mix}} := \frac{g_{YE}g_{EE} + g_{EY}g_{YY}}{\sqrt{g_{EE}^2 + g_{EY}^2}}. \quad (10)$$

As a result, B_μ plays a roll of the ordinary $U(1)_Y$ gauge field, and E_μ is a new gauge field which can have a mass if the B-L symmetry is broken. We use Eq.(9) for the calculations of the RGEs in Appendix A.

The particle contents (except for the gauge bosons) and their charges are presented in Table1. In addition to the SM particles, there are three right-handed neutrinos and a SM singlet complex scalar whose $U(1)_{B-L}$ charge is +2. The relevant terms of the renormalizable Lagrangian are

$$\begin{aligned} \mathcal{L} \supset & -\lambda (H^\dagger H)^2 - \lambda_\Psi (\Psi^\dagger \Psi)^2 - \kappa (H^\dagger H) (\Psi^\dagger \Psi) \\ & - \sum_{ij} y_\nu^{ij} \bar{\nu}_R^i H^\dagger \ell_L^j - \frac{1}{2} \sum_{ij} Y_R^{ij} \bar{\nu}_R^i \nu_R^j \Psi + \text{h.c.} \end{aligned} \quad (11)$$

In the following discussion, we use the bases such that y_ν^{ij} and Y_R^{ij} are real and diagonalized, and assume that they are equal respectively for the three generations. As a result, by including the top mass M_t , there are seven unknown parameters in this model:

$$M_t, \quad g_{B-L}, \quad g_{\text{mix}}, \quad \lambda_\Psi, \quad \kappa, \quad y_\nu, \quad Y_R. \quad (12)$$

If we assume that the small neutrino masses ($\lesssim 1\text{eV}$) are generated by the ordinary seesaw mechanism triggered by the $U(1)_{B-L}$ symmetry breaking at a low energy scale ($\ll 10^{13}$ GeV), y_ν should be very small, and its effects to the RGEs can be negligible. In this paper, we assume such situation.

2.2 Multiple Point Principle

To understand how these couplings behave at a high energy scale, we need to know the RGEs. The two-loop RGEs of this model are presented in Appendix A. Furthermore, the one-loop effective potentials in Landau gauge are as follows⁴:

$$V_{\text{eff}}^H(\mu, \phi) = \frac{\lambda(\mu)}{4} \phi^4 + V_{\text{1loop}}^H(\mu, \phi), \quad V_{\text{eff}}^\Psi(\mu, \Psi) = \frac{\lambda_\Psi(\mu)}{4} \Psi^4 + V_{\text{1loop}}^\Psi(\mu, \Psi), \quad (13)$$

$$\begin{aligned} V_{\text{1loop}}^H(\mu, \phi) := & e^{4\Gamma(\mu)} \left\{ -6 \cdot \frac{M_t(\phi)^4}{64\pi^2} \left[\log \left(\frac{M_t(\phi)^2}{\mu^2} \right) - \frac{3}{2} + 2\Gamma(\mu) \right] \right. \\ & \left. + 6 \cdot \frac{M_W(\phi)^4}{64\pi^2} \left[\log \left(\frac{M_W(\phi)^2}{\mu^2} \right) - \frac{5}{6} + 2\Gamma(\mu) \right] + 3 \cdot \frac{M_Z(\phi)^4}{64\pi^2} \left[\log \left(\frac{M_Z(\phi)^2}{\mu^2} \right) - \frac{5}{6} + 2\Gamma(\mu) \right] \right\} \end{aligned}$$

⁴Here, we neglect the one-loop contributions which include λ , λ_Ψ and κ because their effects are very small when we consider the MPP.

$$V_{\text{1loop}}^\Psi(\mu, \Psi) := e^{4\Gamma_\Psi(\mu)} \left\{ -6 \cdot \frac{M_R(\Psi)^4}{64\pi^2} \left[\log \left(\frac{M_R(\Psi)^2}{\mu^2} \right) - \frac{3}{2} + 2\Gamma_\Psi(\mu) \right] \right. \\ \left. + 3 \cdot \frac{M_{B-L}(\Psi)^4}{64\pi^2} \left[\log \left(\frac{M_{B-L}(\Psi)^2}{\mu^2} \right) - \frac{5}{6} + 2\Gamma_\Psi(\mu) \right] \right\}, \quad (14)$$

where

$$M_t(\phi) = \frac{y_t(\mu)}{\sqrt{2}}\phi \quad , \quad M_W(\phi) = \frac{g_2(\mu)}{2}\phi \quad , \quad M_Z(\phi) = \frac{\sqrt{g_2^2(\mu) + g_Y^2(\mu)}}{2}\phi, \\ M_R(\Psi) = \frac{Y_R(\mu)}{\sqrt{2}}\Psi \quad , \quad M_{B-L}(\Psi)^2 = 2^2 g_{B-L}(\mu)^2 \Psi^2. \quad (15)$$

Here, μ is the renormalization scale and Γ , Γ_Ψ are the wave function renormalizations. To minimize the one-loop contributions, we take $\mu = \phi(\Psi)$ in the following discussion⁵. From these results, we can define the effective self couplings and their effective beta functions as follows:

$$\lambda^{\text{eff}}(\phi) := \frac{4V_{\text{eff}}^H(\phi)}{\phi^4} \quad , \quad \beta_\lambda^{\text{eff}} := \frac{d\lambda^{\text{eff}}(\phi)}{d \ln \phi}, \quad (16)$$

$$\lambda_\Psi^{\text{eff}}(\Psi) := \frac{4V_{\text{eff}}^\Psi(\Psi)}{\Psi^4} \quad , \quad \beta_{\lambda_\Psi}^{\text{eff}} := \frac{d\lambda_\Psi^{\text{eff}}(\Psi)}{d \ln \Psi}. \quad (17)$$

Fig.1 shows the typical behaviors of $\lambda^{\text{eff}}(\phi)$ and its parameter dependences. Here, for the later convenience, the initial values of λ_Ψ , κ , g_{B-L} , g_{mix} and Y_R are given at $\Lambda_{\text{MPP}} = 10^{17}\text{GeV}$, and their typical values are chosen to be 0.1 respectively. One can see that $\lambda^{\text{eff}}(\phi)$ depends weakly on g_{B-L} and Y_R because they appear in β_λ at the two-loop level.

⁵Precisely speaking, μ should be determined as a function of ϕ and Ψ by minimizing the one-loop effective potential. However, in this paper, we simply choose $\mu = \phi(\Psi)$ when we focus on λ^{eff} ($\lambda_\Psi^{\text{eff}}$). It is known that this choice is a good approximation [17].

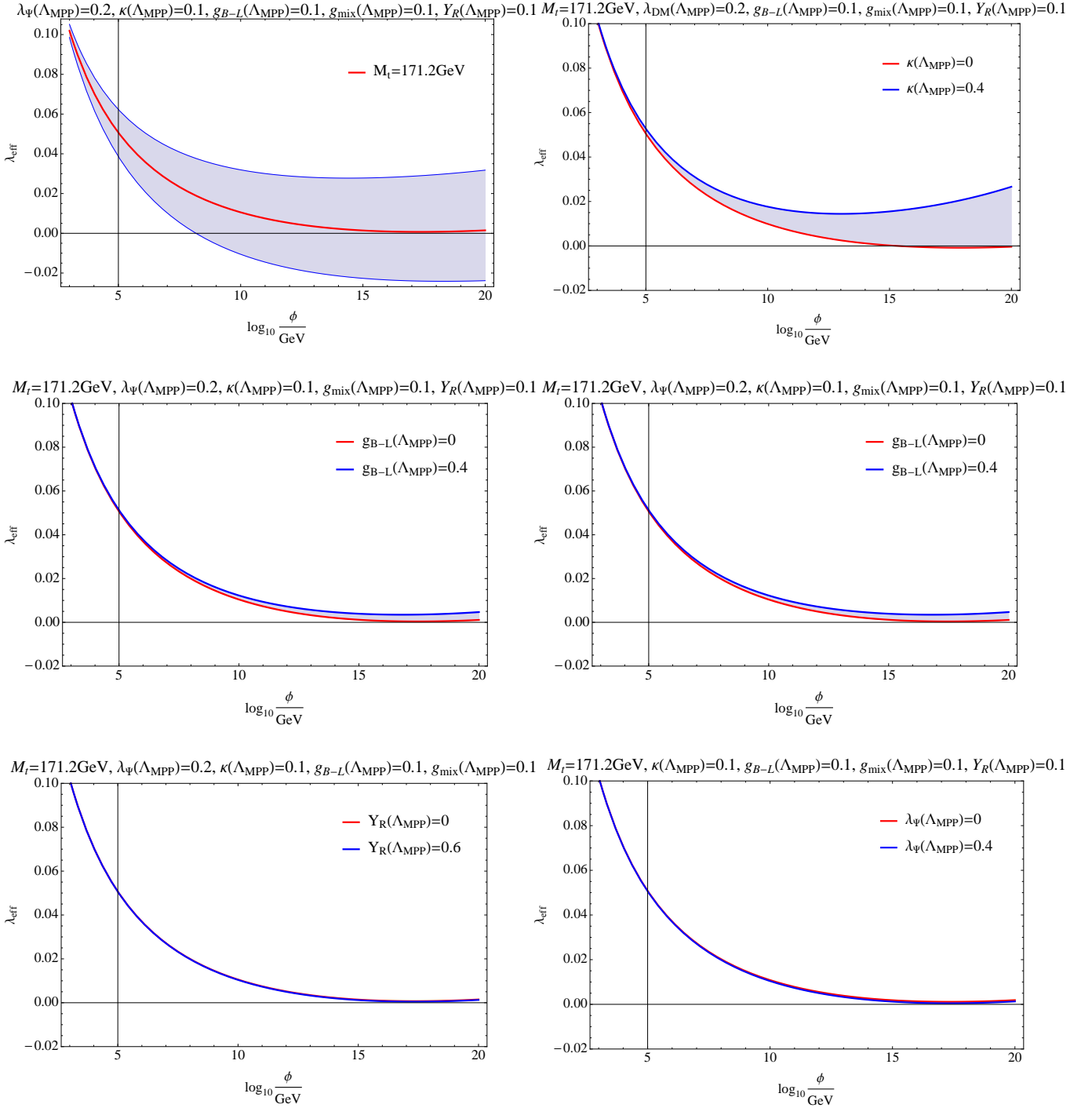


Figure 1: The runnings of the Higgs effective self coupling λ_{eff} as a function of ϕ . The upper left (right) panel shows the M_t ($\kappa(\Lambda_{\text{MPP}})$) dependence. In the case of M_t , the blue band corresponds 95% CL deviation from 171.2GeV. The middle left (right) panel shows the $g_{\text{mix}}(\Lambda_{\text{MPP}})$ ($g_{B-L}(\Lambda_{\text{MPP}})$) dependence. The lower left (right) panel shows the $Y_R(\Lambda_{\text{MPP}})$ ($\lambda_\psi(\Lambda_{\text{MPP}})$) dependence.

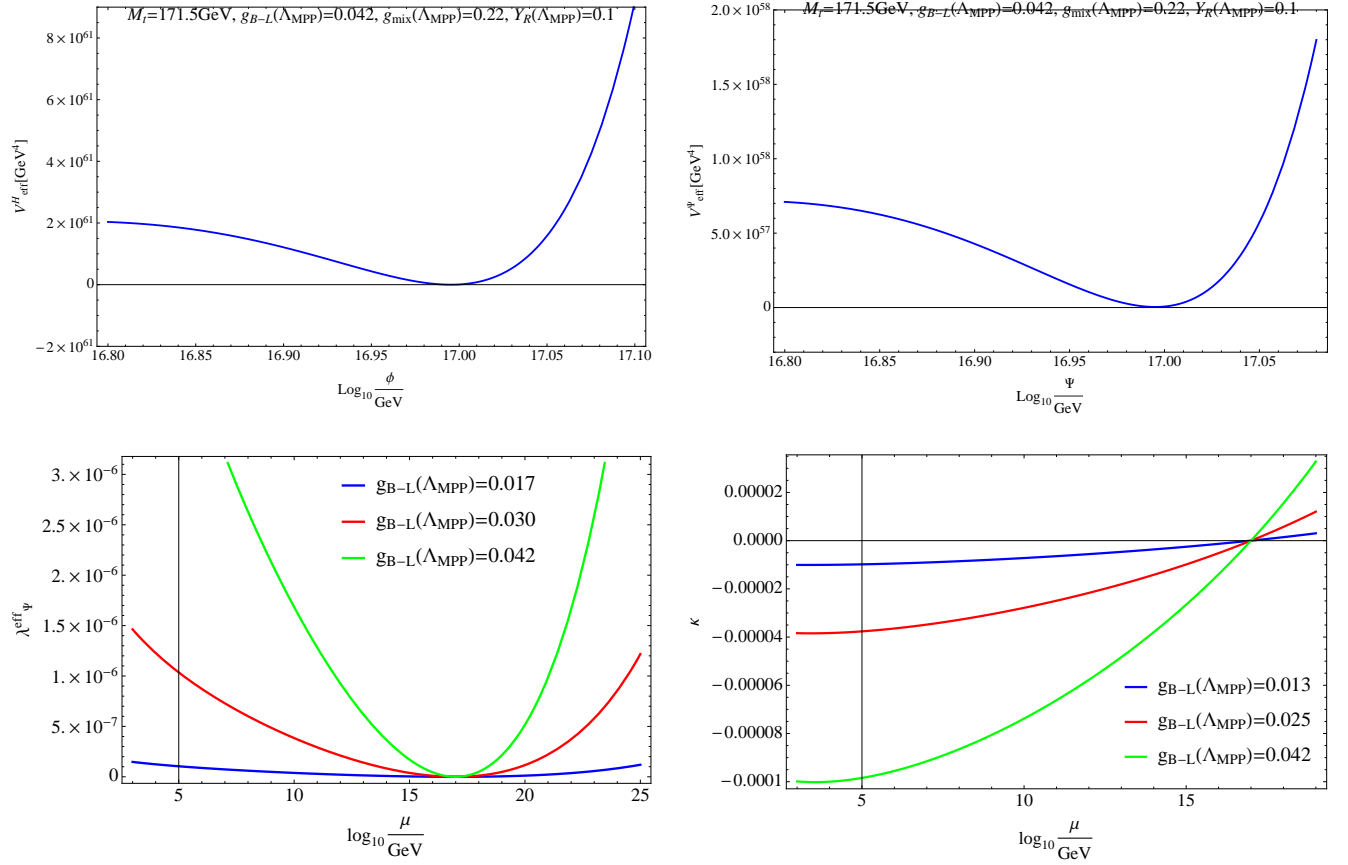


Figure 2: The effective potentials (upper) and the runnings of $\lambda_{\Psi}^{\text{eff}}$ and κ which satisfy the MPP conditions (lower). The upper left (right) panel shows V_{eff}^H (V_{eff}^{Ψ}). They are exactly flat at $\Lambda_{\text{MPP}} = 10^{17}\text{GeV}$. In the lower panels, we leave $g_{B-L}(\Lambda_{\text{MPP}})$ as a free parameter. The different colors correspond to the different values of $g_{B-L}(\Lambda_{\text{MPP}})$.

Now, let us consider the MPP. By including the top mass M_t and neglecting y_{ν} , there are six parameters in this model:

$$M_t, g_{B-L}, g_{\text{mix}}, \lambda_{\Psi}, \kappa, Y_R. \quad (18)$$

Therefore, in principle, they are uniquely determined by the MPP conditions:

$$\lambda_{\Psi}^{\text{eff}}(\Lambda_{\text{MPP}}) = \lambda_{\Psi}^{\text{eff}}(\Lambda_{\text{MPP}}) = \kappa(\Lambda_{\text{MPP}}) = \beta_{\lambda}^{\text{eff}}(\Lambda_{\text{MPP}}) = \beta_{\lambda_{\Psi}}^{\text{eff}}(\Lambda_{\text{MPP}}) = \beta_{\kappa}(\Lambda_{\text{MPP}}) = 0. \quad (19)$$

Among them, $\lambda_{\Psi}^{\text{eff}}(\Lambda_{\text{MPP}}) = \kappa(\Lambda_{\text{MPP}}) = 0$ are just the initial conditions of λ_{Ψ} and κ , and other conditions give us constraints between remaining parameters. We can understand such constraints qualitatively from the one-loop RGEs:

- $\beta_\lambda^{\text{eff}}(\Lambda_{\text{MPP}}) = 0$ mainly relates M_t and g_{mix} because they appear in β_λ at the one-loop level (see Eq.(64) in Appendix A). As a result, we can fix M_t and g_{mix} by $\lambda^{\text{eff}}(\Lambda_{\text{MPP}}) = \beta_\lambda^{\text{eff}}(\Lambda_{\text{MPP}}) = 0$. They are

$$171.62 \text{ GeV} \leq M_t \leq 171.64 \text{ GeV} \quad , \quad 0.18 \leq g_{\text{mix}}(\Lambda_{\text{MPP}}) \leq 0.24 \quad (20)$$

according to $0 \leq g_{B-L}(\Lambda_{\text{MPP}}) \leq 0.4$ ⁶.

- We can obtain a relation between $g_{B-L}(\Lambda_{\text{MPP}})$ and $Y_R(\Lambda_{\text{MPP}})$ by $\beta_{\lambda_\Psi}(\Lambda_{\text{MPP}}) = 0$ because the one-loop part of β_{λ_Ψ} at Λ_{MPP} is

$$\beta_{\lambda_\Psi}|_{1\text{-loop}}(\Lambda_{\text{MPP}}) = \frac{1}{16\pi^2} (96g_{B-L}^4 - 3Y_R^4). \quad (21)$$

- Finally, $g_{B-L}(\Lambda_{\text{MPP}})$ (or $Y_R(\Lambda_{\text{MPP}})$) is fixed at 0 by $\beta_\kappa(\Lambda_{\text{MPP}}) = 0$ because the one-loop part of β_κ at Λ_{MPP} is

$$\beta_\kappa|_{1\text{-loop}}(\Lambda_{\text{MPP}}) = \frac{1}{16\pi^2} (12g_{B-L}^2g_{\text{mix}}^2 - 12Y_R^2y_\nu^2) \simeq \frac{12g_{B-L}^2g_{\text{mix}}^2}{16\pi^2}. \quad (22)$$

In Fig.2, we show the effective potentials (upper) and the runnings (lower) of $\lambda_\Psi^{\text{eff}}$ and κ which satisfy the above MPP conditions. Here, in the lower panels, we leave $g_{B-L}(\Lambda_{\text{MPP}})$ as a free parameter. One can see that the flat potentials can be actually realized at Λ_{MPP} .

Summary : From the MPP at $\Lambda_{\text{MPP}} = 10^{17}\text{GeV}$, the parameters of the gauged B-L extension of the SM are fixed at

$$\begin{aligned} M_t &\simeq 171.6\text{GeV} \quad , \quad g_{B-L}(\Lambda_{\text{MPP}}) \simeq 0 \quad , \quad g_{\text{mix}}(\Lambda_{\text{MPP}}) \simeq 0.24 \quad , \\ \lambda_\Psi(\Lambda_{\text{MPP}}) &\simeq 0 \quad , \quad \kappa(\Lambda_{\text{MPP}}) \simeq 0 \quad , \quad Y_R(\Lambda_{\text{MPP}}) \simeq 0. \end{aligned} \quad (23)$$

2.3 Electroweak Symmetry Breaking by Breaking the MPP

We first explain how the electroweak symmetry breaking is triggered by the B-L symmetry breaking. If Ψ has an expectation value $\langle \Psi \rangle := v_{B-L}/\sqrt{2}$, the interaction term $-\kappa(H^\dagger H)(\Psi^\dagger \Psi)$ produces the mass term of H :

$$\mathcal{L} \ni -\frac{\kappa}{2}v_{B-L}^2H^\dagger H. \quad (24)$$

Thus, if κ is negative at the B-L breaking scale, the electroweak symmetry breaking occurs, and the corresponding Higgs expectation value v_h is given by

$$v_h = \sqrt{-\frac{\kappa}{2\lambda}} \times v_{B-L} \Big|_{\mu=v_h}. \quad (25)$$

⁶ $Y_R(\Lambda_{\text{MPP}})$ dependence is negligible.

This is a relation between v_h and v_{B-L} . We must consider a few questions to realize the electroweak symmetry breaking $\mathcal{O}(100)\text{GeV}$:

Question1 : Does the B-L symmetry breaking actually occur? Especially, is it possible to realize it under the situation where the MPP is exactly satisfied ?

See the lower left panel of Fig.2 once again. This shows the running of $\lambda_{\Psi}^{\text{eff}}$ when the MPP conditions are satisfied. One can see that $\lambda_{\Psi}^{\text{eff}}$ is a simply decreasing function. Thus, we can not obtain the B-L symmetry breaking if the MPP is realized exactly. However, as discussed in [26], the situation changes when $\lambda_{\Psi}^{\text{eff}}(\Lambda_{\text{MPP}}) > 0$, which means the breaking of the MPP. See the upper and middle left panels of Fig.3. They show the runnings of $\lambda_{\Psi}^{\text{eff}}$ when $\lambda_{\Psi}^{\text{eff}}(\Lambda_{\text{MPP}}) = 10^{-10}$ and 10^{-12} respectively⁷. One can see that $\lambda_{\Psi}^{\text{eff}}$ can cross zero, and its scale strongly depends on $g_{B-L}(\Lambda_{\text{MPP}})$. For convenience, we also show the corresponding effective potentials of Ψ in the upper and middle right panels. Here, we have normalized the vertical axes so that the minimums of the potentials can be easily understood.

Question2 : Although we have seen that the B-L symmetry breaking is possible if we break the MPP, is it possible to realize $v_h = \mathcal{O}(100)\text{GeV}$?

To answer this question, we should know the typical values of κ at a low energy scale (see Eq.(25)). Before seeing the numerical results, let us understand it qualitatively. Because we now focus on the MPP, the one-loop part of β_{κ} approximately becomes (see Eq.(65) in Appendix A)

$$\beta_{\kappa}|_{1\text{-loop}} \simeq \frac{12g_{B-L}^2 g_{\text{mix}}^2}{16\pi^2} \simeq \frac{g_{B-L}^2}{\pi} \times 10^{-2}, \quad (26)$$

where we have used $g_{\text{mix}} \simeq 0.2$ which was obtained in the previous subsection. Thus, κ at a low energy scale μ is approximately given by

$$-\kappa(\mu) = c \times 0.1 \times g_{B-L}^2(\mu), \quad (27)$$

where c is a constant and we have used the fact that g_{B-L} does not so change. This is the qualitative expression of $\kappa(\mu)$. In the lower left (right) panel of Fig.3, we show κ vs g_{B-L} at $\mu = M_t = 171.6\text{GeV}$ for $\lambda_{\Psi}^{\text{eff}}(\Lambda_{\text{MPP}}) = 10^{-10}$ (10^{-12}). One can see that Eq.(27) nicely explains the numerical results when c is 0.70. As a result, v_h is given by

$$v_h = \sqrt{\frac{0.1 \times c \times g_{B-L}(v_h)^2}{2\lambda(v_h)}} \times v_{B-L} \simeq g_{B-L}(v_h)v_{B-L}, \quad (28)$$

⁷In Section 3, we will see that the smallness of $\lambda_{\Psi}^{\text{eff}}$ is needed to realize the inflation consistently. That's why we have chosen $\lambda_{\Psi}^{\text{eff}}$ so small here.

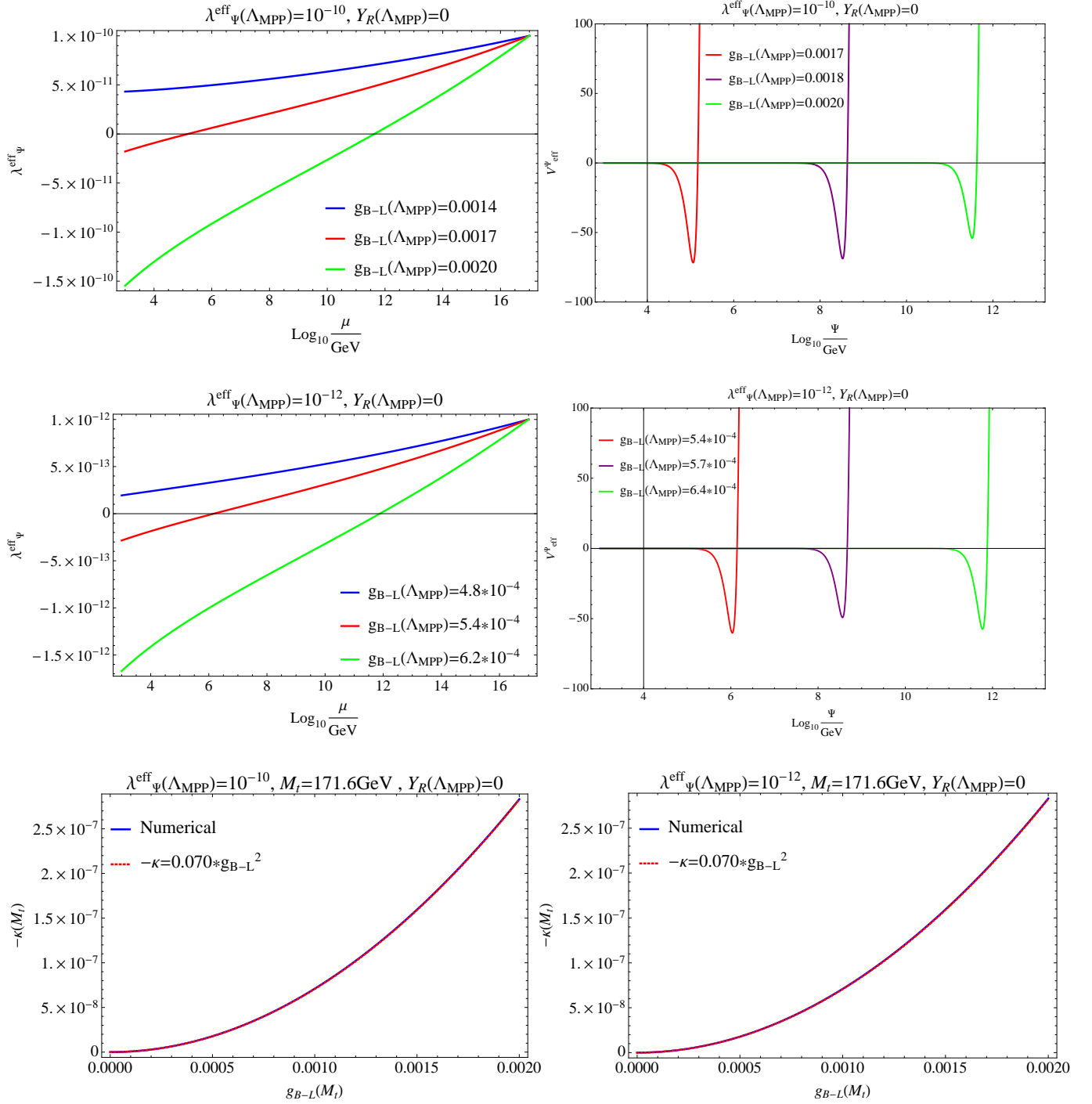


Figure 3: Upper (Middle): the runnings of $\lambda_{\Psi}^{\text{eff}}$ (left) and the corresponding effective potentials (right) in the case of $\lambda_{\Psi}^{\text{eff}}(\Lambda_{\text{MPP}}) = 10^{-10}$ (10^{-12}). Here, the vertical axes of the right panels are properly normalized. The different colors correspond to the different values of $g_{B-L}(\Lambda_{\text{MPP}})$. Lower left (right): κ vs g_{B-L} at $M_t = 171.6 \text{ GeV}$ for $\lambda_{\Psi}^{\text{eff}}(\Lambda_{\text{MPP}}) = 10^{-10}$ (10^{-12}). Here, the solid blue lines are the numerical results of the RGEs, and the dashed red contours represent $-\kappa = 0.070 \times g_{B-L}^2$.

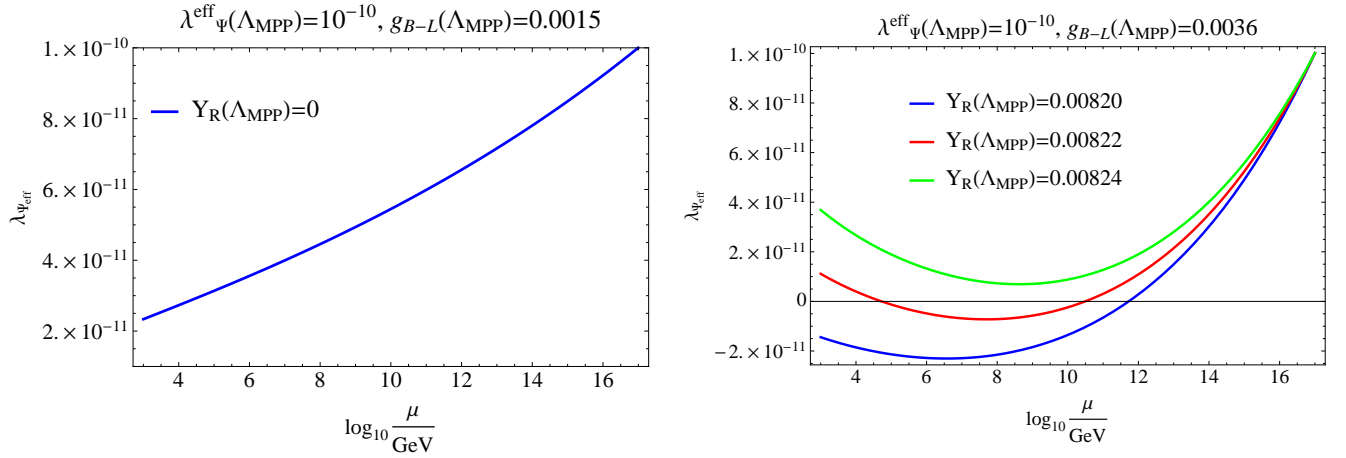


Figure 4: The impossibility to realize $v_h = \mathcal{O}(100)\text{GeV}$ when $g_{B-L}(\Lambda_{\text{MPP}})$ is outside the region given by Eq.(29). The left (right) panel shows the running of $\lambda_{\Psi}^{\text{eff}}$ when $g_{B-L}(\Lambda_{\text{MPP}}) = 0.0015$ (0.0036). In the left panel, one can see that $\lambda_{\Psi}^{\text{eff}}$ is always positive even if $Y_R(\Lambda_{\text{MPP}}) = 0$. In the right panel, one can see that B-L symmetry breaking occurs at a very high energy scale ($\gg 10^2$ TeV).

where we have used the typical value $\lambda(v_h) \simeq 0.1$. Therefore, we can obtain $v_h = \mathcal{O}(100)\text{GeV}$ by tuning $g_{B-L}(\Lambda_{\text{MPP}})$ and $Y_R(\Lambda_{\text{MPP}})$ so that the right hand side of Eq.(28) becomes $\mathcal{O}(100)\text{GeV}$. The red lines of the upper and middle left panels of Fig.3 represent such examples. In the upper (lower) case, g_{B-L} is $\mathcal{O}(10^{-3}(10^{-4}))$ and v_{B-L} is $\mathcal{O}(10^2(10^3))\text{TeV}$.

A few comments are needed. First, because we no longer impose the flatness of V_{eff}^{Ψ} , the two parameters $g_{B-L}(\Lambda_{\text{MPP}})$ and $Y_R(\Lambda_{\text{MPP}})$ are remaining as free parameters. However, the parameter region which can produce $v_h = \mathcal{O}(100)\text{GeV}$ is quite limited. For example, in the $\lambda_{\Psi}^{\text{eff}}(\Lambda_{\text{MPP}}) = 10^{-10}$ case, it is

$$1.6 \times 10^{-3} \lesssim g_{B-L}(\Lambda_{\text{MPP}}) \lesssim 3.5 \times 10^{-3}, \quad (29)$$

and $Y_R(\Lambda_{\text{MPP}})$ is correspondingly fixed so that $\lambda_{\Psi}^{\text{eff}}$ crosses zero around $\mathcal{O}(100)\text{TeV}$. The reason is as follows. When $g_{B-L}(\Lambda_{\text{MPP}})$ is small, $\beta_{\lambda_{\Psi}}$ is too small to make $\lambda_{\Psi}^{\text{eff}}$ negative at a low energy scale. As a result, the B-L symmetry breaking does not occur. On the other hand, when $g_{B-L}(\Lambda_{\text{MPP}})$ is too large, the B-L symmetry breaking occurs at a very high energy scale. We can actually see these behaviors from Fig.4. Note that the allowed values of $g_{B-L}(\Lambda_{\text{MPP}})$ become small when we decrease $\lambda_{\Psi}^{\text{eff}}(\Lambda_{\text{MPP}})$.

Second, g_{B-L} at a low energy scale does not so change from the value at Λ_{MPP} . See Fig.5. This shows the typical runnings of g_{B-L} when $\lambda_{\Psi}^{\text{eff}}(\Lambda_{\text{MPP}}) = 10^{-10}$.

Finally, when the MPP of the Higgs potential is realized, the mass of the B-L gauge

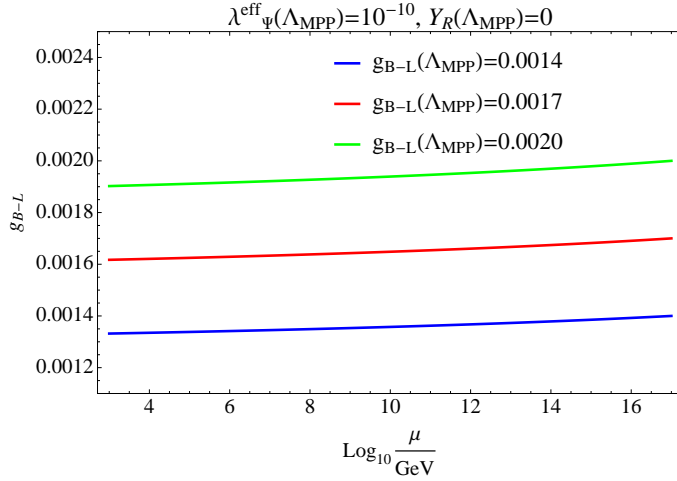


Figure 5: The typical runnings of g_{B-L} when $\lambda_{\Psi}^{\text{eff}}(\Lambda_{\text{MPP}}) = 10^{-10}$.

boson is uniquely predicted to be

$$M_{B-L} = 2g_{B-L}(v_{B-L})v_{B-L} = 3.4 \times \sqrt{\frac{\lambda(v_h)}{0.10}} \times v_h, \quad (30)$$

where we have used Eq.(28) and $c = 0.70$. By using the experimental value $v_h = 246\text{GeV}$ and the typical value $\lambda(v_h) \simeq 0.1$, this leads to

$$M_{B-L} \simeq 836 \text{ GeV}. \quad (31)$$

Although this is a remarkable prediction of the MPP, this value is already excluded by the experiment of ATLAS [29] because g_{mix} is too large⁸.

3 Non-Minimal Inflation - SM Singlet Scalar as the Inflaton -

As is well known, the Higgs inflation is possible in the SM [14, 15, 16, 17, 18]. There, the criticality of the Higgs potential plays a crucial role to realize the inflation naturally; we can obtain a sufficient e-foldings and the CMB fluctuations even if ξ is $\mathcal{O}(1)$ by making the running Higgs self coupling arbitrary small (see [17] for more details). In other words, the smallness of the self coupling is needed to realize the inflation naturally. Such a Higgs inflation is of course possible in our B-L model, however, the conclusion

⁸In [29], g_{mix} is represented by \tilde{g}_Y . Therefore, $g_{\text{mix}} \simeq 0.24$ corresponds to the contour $\gamma' \simeq 0.32/\sin\theta$ in FIG.7 of [29].

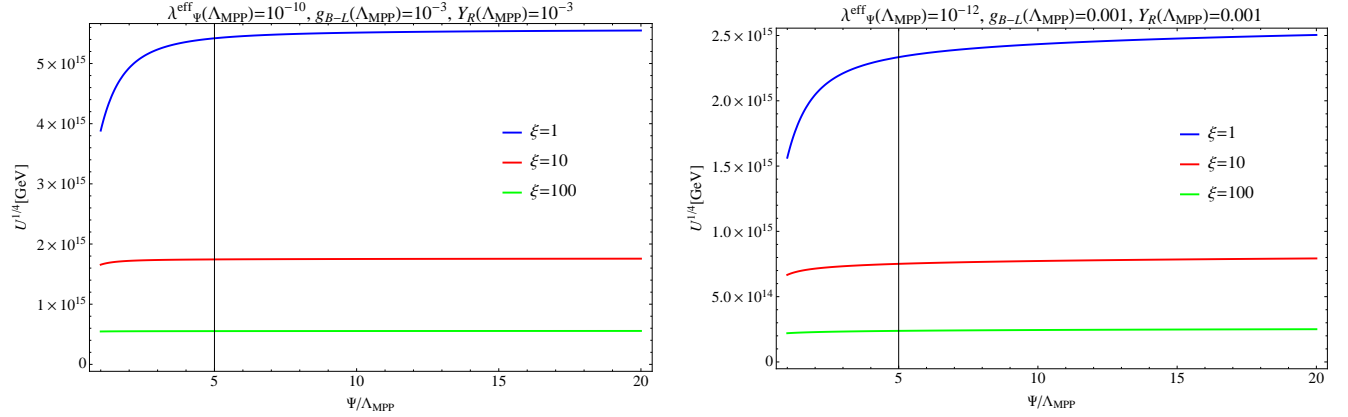


Figure 6: The effective potentials in the Einstein frame. The left (right) panel shows the $\lambda_{\Psi}^{\text{eff}}(\Lambda_{\text{MPP}}) = 10^{-10}$ (10^{-12}) case. The different colors correspond to the different values of ξ .

of the previous section indicates a new possibility: The newly introduced SM singlet complex scalar Ψ plays a roll of the inflaton [28]. We study this scenario in this section.

The action with the non-minimal gravitational coupling $\xi\Psi^2\mathcal{R}$ in the Jordan frame is given by

$$S_J = \int d^4x \sqrt{-g} \left\{ - \left(\frac{M_{pl}^2 + \xi\Psi^2}{2} \right) \mathcal{R} + \frac{1}{2} g^{\mu\nu} \partial_\mu \Psi \partial_\nu \Psi - \frac{\lambda_{\Psi}^{\text{eff}}(\Psi)}{4} \Psi^4 + \dots \right\}, \quad (32)$$

where Ψ is the physical (real) field, and we have written the relevant terms for the later discussion. To study the inflation, it is convenient to move to the Einstein frame. Namely, by the conformal transformation

$$g_{\mu\nu}^E := \Omega^2 g_{\mu\nu}, \quad \Omega^2 := 1 + \frac{\xi\Psi^2}{M_{pl}^2}, \quad (33)$$

and the field redefinition

$$\frac{d\chi}{d\Psi} = \sqrt{\frac{\Omega^2 + 6\xi^2\Psi^2/M_{pl}^2}{\Omega^4}}, \quad (34)$$

the action becomes

$$S_E = \int d^4x \sqrt{-g_E} \left\{ - \frac{M_{pl}^2}{2} \mathcal{R}_E + \frac{1}{2} g_E^{\mu\nu} \partial_\mu \chi \partial_\nu \chi - \frac{\lambda_{\Psi}^{\text{eff}}(\Psi)}{4\Omega^4} \Psi^4(\chi) + \dots \right\}. \quad (35)$$

This is the canonically normalized form, and the potential in this frame is given by

$$U(\chi) := \frac{\lambda_{\Psi}^{\text{eff}}(\Psi)}{4\Omega^4} \Psi^4(\chi). \quad (36)$$

For the large values of $\Psi \gg M_{pl}/\sqrt{\xi}$, Eq.(34) becomes

$$\frac{d\chi}{d\Psi} \simeq \frac{M_{pl}}{\Psi} \sqrt{\frac{1+6\xi}{\xi}}, \quad (37)$$

so we have

$$\Psi \simeq M_{pl} \exp\left(\frac{\chi}{M_{pl}\sqrt{(1+6\xi)/\xi}}\right). \quad (38)$$

In this limit, the potential in the Einstein frame Eq.(36) becomes

$$U(\chi) \simeq \frac{\lambda_{\Psi}^{\text{eff}}(\Psi)M_{pl}^4}{4\xi^2} \left(1 + \exp\left(-\frac{2\chi}{M_{pl}\sqrt{(1+6\xi)/\xi}}\right)\right)^{-2}. \quad (39)$$

This is an exponentially flat potential (see Fig.(6) for example), so we can use the slow-roll approximations. The slow-roll parameters are

$$\epsilon := \frac{M_{pl}^2}{2} \left(\frac{1}{U} \frac{dU}{d\chi}\right)^2 = \frac{M_{pl}^2}{2} \left(\frac{d\Psi}{d\chi} \frac{U'}{U}\right)^2, \quad (40)$$

$$\eta := M_{pl}^2 \left(\frac{1}{U} \frac{d^2U}{d\chi^2}\right) = \frac{M_{pl}^2}{U} \frac{d\Psi}{d\chi} \frac{d}{d\Psi} \left(\frac{d\Psi}{d\chi} U'\right), \quad (41)$$

$$\zeta := M_{pl}^4 \frac{1}{U} \frac{d^3U}{d\chi^3} \frac{dU}{d\chi}, \quad (42)$$

where a prime represents a derivative with respect to Ψ . By using these quantities, the number of e-foldings N , the spectral index n_s , its running $dn_s/d \ln k$ and the tensor-to-scalar ratio r are given by

$$N = \int_{\chi_{end}}^{\chi_{ini}} d\chi \frac{1}{M_{pl}^2} \frac{U}{dU/d\chi} = \int_{\Psi_{end}}^{\Psi_{ini}} d\Psi \frac{1}{M_{pl}^2} \frac{U}{U'} \quad (43)$$

$$n_s = 1 - 6\epsilon + 2\eta, \quad (44)$$

$$\frac{dn_s}{d \ln k} = 16\epsilon\eta - 24\epsilon^2 - 2\zeta^2, \quad (45)$$

$$r = 16\epsilon, \quad (46)$$

where Ψ_{ini} (Ψ_{end}) represents the initial (end) value of Ψ . In the following discussion, we denote Ψ_{ini} simply as Ψ .

Here, we give the current cosmological constraints by Planck TT + lowP [32]. The overall normalization of the CMB fluctuations at the scale $k_0 = 0.05 \text{ Mpc}^{-1}$ is

$$A_s := \frac{U}{24\pi^2 \epsilon M_{pl}^4} \Big|_{k_0} = (2.198_{-0.085}^{+0.076}) \times 10^{-9} \quad (68\% \text{ CL}), \quad (47)$$

and n_s , $dn_s/d \ln k$ and r are

$$n_s = 0.9655 \pm 0.0062 \text{ (68\% CL)}, \quad \frac{dn_s}{d \ln k} = -0.0126_{-0.0087}^{+0.0098} \text{ (68\% CL)}, \quad r_{0.002} < 0.10 \text{ (95\% CL)}, \quad (48)$$

at the scale $k_0 = 0.05 \text{ Mpc}^{-1}$ for n_s and $dn_s/d \ln k$, and $k_r = 0.002 \text{ Mpc}^{-1}$ for $r_{0.002}$. On the other hand, the BICEP2 experiment has reported an observation of $r_{0.002}$ [33]:

$$r_{0.002} = 0.20_{-0.05}^{+0.07} \text{ (68\% CL)}. \quad (49)$$

There has been discussion such that this result may be consistent with $r = 0$ due to the foreground effect [34, 35].

Our calculations are based on the following conditions:

1. Although there are six parameters, we consider the situation where M_t and g_{mix} are fixed so that the Higgs potential $V_{\text{eff}}^H(\phi)$ becomes flat at $\Lambda_{\text{MPP}} = 10^{17} \text{ GeV}$ in addition to $\kappa(\Lambda_{\text{MPP}}) = 0$.
2. As the typical values of $\lambda_{\Psi}^{\text{eff}}(\Lambda_{\text{MPP}})$, we choose

$$\lambda_{\Psi}^{\text{eff}}(\Lambda_{\text{MPP}}) = 10^{-10}, 10^{-12} \text{ and } 10^{-14}. \quad (50)$$

3. The two parameters $g_{B-L}(\Lambda_{\text{MPP}})$ and $Y_R(\Lambda_{\text{MPP}})$ are chosen so that v_h becomes $\mathcal{O}(100) \text{ GeV}$. As discussed at the end of Section 2, the allowed region is quite limited in this case. We have checked that the cosmological predictions do not so change even if we change these parameters within such region (see Fig.8).

Fig.7 shows the results when we fix $g_{B-L}(\Lambda_{\text{MPP}})$ and $Y_R(\Lambda_{\text{MPP}})$. Our results are, of course, consistent with the previous results such as [28, 36]. The left (right) panels show r ($dn_s/\ln k$) vs n_s . Here, the solid blue (red) lines represent $\xi(\Psi) = \text{constant}$, and the contours which correspond to $N = 50$ and 60 are represented by orange and black respectively from $\xi = 0$ to $\xi = 100$. In the left panels, we also show the contours which correspond to the observed value of A_s by green from $\xi = 0$ to $\xi = 100$. These results are consistent with the observed results (48)(49) by Planck and BICEP2. Especially, as one can see from the behaviors of the green lines, the values of $\lambda_{\Psi}^{\text{eff}}(\Lambda_{\text{MPP}})$ which can simultaneously explain $A_s = 2.19 \times 10^{-9}$, the sufficient e-foldings ($N \geq 50$) and the BICEP2's result $r = 0.2$ are quite limited:

$$10^{-14} < \lambda_{\Psi}^{\text{eff}}(\Lambda_{\text{MPP}}) < 10^{-12}. \quad (51)$$

Among the three quantities n_s , r and $dn_s/\ln k$, one might think that the predicted values of $dn_s/\ln k$ are small compared with the observed values $\mathcal{O}(-0.01)$. We may improve this situation by including a higher dimensional operator. See [17] for example.

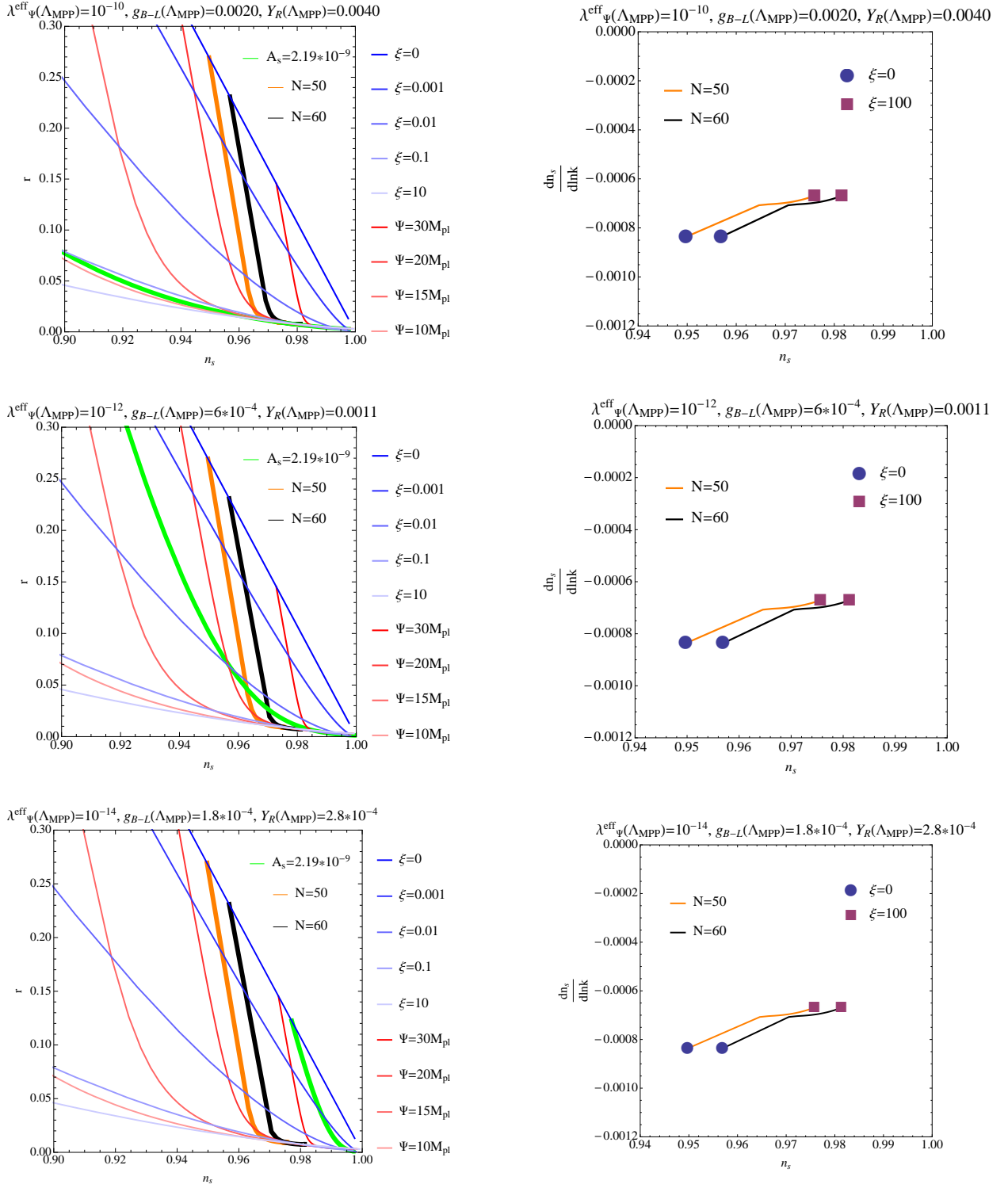


Figure 7: The cosmological predictions of the gauged B-L model. The upper, middle and lower panels correspond to $\lambda_{\Psi}^{\text{eff}}(\Lambda_{\text{MPP}}) = 10^{-10}$, 10^{-12} and 10^{-14} respectively. The left (right) panels show n_s vs r ($dn_s/d\ln k$). The blue (red) lines indicate ξ (Ψ) = constant, and the contours which correspond to $N = 50$ and 60 are represented by orange and black respectively.

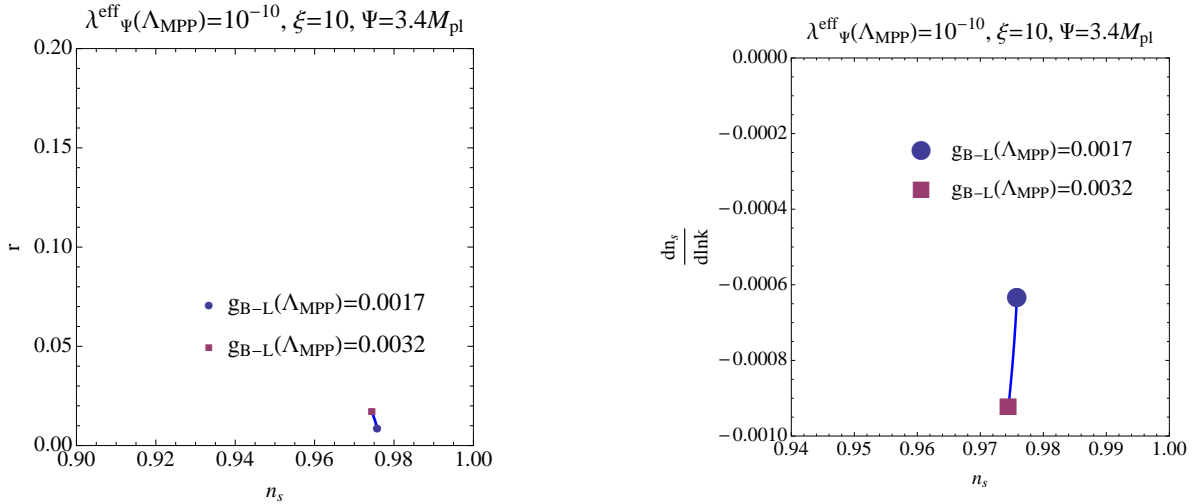


Figure 8: The $g_{B-L}(\Lambda_{\text{MPP}})$ dependences of n_s , r and $dn_s/\ln k$. Here, we change $g_{B-L}(\Lambda_{\text{MPP}})$ within the region such that the electroweak symmetry breaking occurs at $\mathcal{O}(100)\text{GeV}$, and ξ and Ψ are chosen so that both of the observed value of A_s and $N = 50$ are satisfied when $g_{B-L}(\Lambda_{\text{MPP}}) = 0.0020$. The left (right) panel shows r ($dn_s/\ln k$) vs n_s .

In Fig.8, we also show how n_s , r and $dn_s/\ln k$ depend on $g_{B-L}(\Lambda_{\text{MPP}})$ when $\lambda_{\Psi}^{\text{eff}}(\Lambda_{\text{MPP}}) = 10^{-10}$. Here, we change $g_{B-L}(\Lambda_{\text{MPP}})$ within the region such that the electroweak symmetry breaking occurs at $\mathcal{O}(100)\text{GeV}$. Furthermore, Ψ and ξ are chosen so that they explain both of the observed value of A_s and $N = 50$ when $g_{B-L}(\Lambda_{\text{MPP}}) = 0.0020$. One can see that n_s and r hardly depend on $g_{B-L}(\Lambda_{\text{MPP}})$ and that the change of $dn_s/\ln k$ is at most $\mathcal{O}(0.0001)$. As a result, under the situation where the Higgs potential is flat at Λ_{MPP} and that the electroweak symmetry breaking occurs at $\mathcal{O}(100)\text{GeV}$, the gauged B-L model uniquely predicts the cosmological observables. This is also one of the benefits of the (slightly broken) MPP.

4 Summary

In this paper, we have considered the MPP and the inflation of the gauged B-L extension of the SM. We have found that the scalar couplings and their beta functions can simultaneously become zero at $\Lambda_{\text{MPP}} = 10^{17}\text{GeV}$ and that the parameters of the model can be uniquely fixed by this conditions. However, from the point of view that the electroweak symmetry breaking should be realized by the radiatively broken B-L symmetry, it is necessary to break the MPP; we need $\lambda_{\Psi}^{\text{eff}}(\Lambda_{\text{MPP}}) > 0$. In subsection 2.3, we found that the small values of $\lambda_{\Psi}^{\text{eff}}(\Lambda_{\text{MPP}})$ are compatible with the electroweak symmetry breaking at $\mathcal{O}(100)\text{GeV}$. Especially, we have found that the mass of the B-L

gauge boson can be predicted to be

$$M_{B-L} = 3.4 \times \sqrt{\frac{\lambda(v_h)}{0.10}} \times v_h \quad (52)$$

from the MPP of the Higgs potential and κ . This is one of the remarkable predictions of the MPP. In Section 3, we have studied the inflation where the SM singlet scalar Ψ plays a roll of the inflaton. We have calculated the cosmological observables based on the assumptions that the Higgs potential is flat at $\Lambda_{\text{MPP}} = 10^{17}\text{GeV}$ and the $\mathcal{O}(100)\text{GeV}$ electroweak symmetry breaking occurs. The results in this paper are consistent with the observations by Planck and BICEP2. Among them, the predicted values of the running of the special index $dn_s/\ln k$ are small compared with the observed values $\mathcal{O}(-0.01)$. Thus, it might be interesting to consider whether we can improve this situation. One of the such possibilities is to include a higher dimensional operator [17]. In conclusion, the gauged B-L extension of the SM is a phenomenologically very interesting model in that it can explain both of the cosmological observations and the electroweak symmetry breaking at $\mathcal{O}(100)\text{GeV}$ simultaneously by breaking the MPP.

Acknowledgement

We thank Hikaru Kawai and Yuta Hamada for valuable discussions.

Appendix A Two-Loop Renormalization Group Equations

The two-loop RGEs of the gauged B-L model are as follows⁹:

$$\frac{d\Gamma_H}{dt} = \frac{1}{(4\pi)^2} \left(\frac{9}{4}g_2^2 + \frac{3}{4}g_Y^2 + \frac{3}{4}g_{\text{mix}}^2 - 3y_t^2 - 3y_\nu^2 \right), \quad (53)$$

$$\frac{d\Gamma_\Psi}{dt} = \frac{1}{(4\pi)^2} \left(12g_{B-L}^2 - \frac{3}{2}Y_R^2 \right), \quad (54)$$

$$\begin{aligned} \frac{dg_Y}{dt} = \frac{1}{(4\pi)^2} \frac{41}{6}g_Y^3 + \frac{g_Y^3}{(4\pi)^4} & \left(\frac{199}{18}g_Y^2 + \frac{9}{2}g_2^2 + \frac{44}{3}g_3^2 + \frac{92}{9}g_{B-L}^2 + \frac{199}{18}g_{\text{mix}}^2 \right. \\ & \left. + \frac{164}{9}g_{\text{mix}}g_{B-L} - \frac{17}{6}y_t^2 - \frac{3}{2}y_\nu^2 \right), \end{aligned} \quad (55)$$

⁹Our calculations are based on [37, 38, 39, 40]. Especially, the two-loop results with an arbitrary number of Abelian groups are presented in [40].

$$\begin{aligned}
\frac{dg_{\text{mix}}}{dt} = & \frac{1}{(4\pi)^2} \left(\frac{41}{6} g_{\text{mix}} (g_{\text{mix}}^2 + 2g_Y^2) + \frac{32}{3} g_{B-L} (g_{\text{mix}}^2 + g_Y^2) + 12g_{\text{mix}}g_{B-L}^2 \right) \\
& + \frac{1}{(4\pi)^4} \left\{ g_{\text{mix}}^3 \left(\frac{199}{18} g_{\text{mix}}^2 + \frac{328}{9} g_{\text{mix}}g_{B-L} + \frac{9}{2} g_2^2 + \frac{44}{3} g_3^2 + \frac{184}{3} g_{B-L}^2 + \frac{199}{6} g_Y^2 \right) \right. \\
& + g_{\text{mix}}^2 \left(\frac{656}{9} g_Y^2 g_{B-L} + \frac{448}{9} g_{B-L}^3 + \frac{32}{3} g_3^2 g_{B-L} + 12g_2^2 g_{B-L} \right) \\
& + g_{\text{mix}} \left(\frac{644}{9} g_Y^2 g_{B-L}^2 + \frac{800}{9} g_{B-L}^4 + 12g_2^2 g_{B-L}^2 + \frac{199}{9} g_Y^4 + 9g_2^2 g_Y^2 + \frac{88}{3} g_3^2 g_Y^2 + \frac{32}{3} g_3^2 g_{B-L}^2 \right) \\
& + \frac{164}{9} g_Y^4 g_{B-L} + \frac{224}{9} g_Y^2 g_{B-L}^3 + 12g_2^2 g_Y^2 g_{B-L} + \frac{32}{3} g_3^2 g_Y^2 g_{B-L} \\
& - y_t^2 \left(\frac{10}{3} g_Y^2 g_{B-L} + \frac{17}{6} g_{\text{mix}}^3 + \frac{10}{3} g_{\text{mix}}^2 g_{B-L} + \frac{4}{3} g_{\text{mix}} g_{B-L}^2 + \frac{17}{3} g_{\text{mix}} g_Y^2 \right) \\
& \left. - y_\nu^2 \left(6g_Y^2 g_{B-L} + \frac{3}{2} g_{\text{mix}}^3 + 3g_{\text{mix}} g_Y^2 + 6g_{\text{mix}}^2 g_{B-L} + 12g_{\text{mix}} g_{B-L}^2 \right) - 3Y_R^2 g_{\text{mix}} g_{B-L}^2 \right\}, \tag{56}
\end{aligned}$$

$$\begin{aligned}
\frac{dg_{B-L}}{dt} = & \frac{g_{B-L}}{(4\pi)^2} \left(12g_{B-L}^2 + \frac{32}{3} g_{B-L} g_{\text{mix}} + \frac{41}{6} g_{\text{mix}}^2 \right) \\
& + \frac{g_{B-L}}{(4\pi)^4} \left\{ g_{B-L}^2 \left(\frac{800}{9} g_{B-L}^2 + \frac{92}{9} g_y^2 + \frac{184}{3} g_{\text{mix}}^2 + 12g_2^2 + \frac{32}{3} g_3^2 + \frac{448}{9} g_{\text{mix}} g_{B-L} \right) \right. \\
& + g_{B-L} \left(\frac{164}{9} g_{\text{mix}} g_y^2 + \frac{328}{9} g_{\text{mix}}^3 + 12g_2^2 g_{\text{mix}} + \frac{32}{3} g_3^2 g_{\text{mix}} \right) \\
& + \frac{199}{18} g_{\text{mix}}^2 g_y^2 + \frac{199}{18} g_{\text{mix}}^4 + \frac{9}{2} g_2^2 g_{\text{mix}}^2 + \frac{44}{3} g_3^2 g_{\text{mix}}^2 \\
& \left. - y_t^2 \left(\frac{4}{3} g_{B-L}^2 + \frac{10}{3} g_{\text{mix}} g_{B-L} + \frac{17}{6} g_{\text{mix}}^2 \right) - y_\nu^2 \left(6g_{\text{mix}} g_{B-L} - \frac{3}{2} g_{\text{mix}}^2 - 12g_{B-L}^2 \right) - 3Y_R^2 g_{B-L}^2 \right\}, \tag{57}
\end{aligned}$$

$$\frac{dg_2}{dt} = -\frac{1}{(4\pi)^2} \frac{19}{6} g_3^2 + \frac{g_2^3}{(4\pi)^4} \left(\frac{3}{2} g_Y^2 + \frac{35}{6} g_2^2 + 12g_3^2 + 4g_{B-L}^2 + \frac{3}{2} g_{\text{mix}}^2 + 4g_{\text{mix}} g_{B-L} - \frac{3}{2} y_t^2 - \frac{3}{2} y_\nu^2 \right), \tag{58}$$

$$\frac{dg_3}{dt} = -\frac{7}{(4\pi)^2} g_3^3 + \frac{g_3^3}{(4\pi)^4} \left(\frac{11}{6} g_Y^2 + \frac{9}{2} g_2^2 - 26g_3^2 + \frac{4}{3} g_{B-L}^2 + \frac{11}{6} g_{\text{mix}}^2 + \frac{4}{3} g_{\text{mix}} g_{B-L} - 2y_t^2 \right), \tag{59}$$

$$\begin{aligned}
\frac{dy_t}{dt} = & \frac{y_t}{(4\pi)^2} \left(\frac{9}{2}y_t^2 + 3y_\nu^2 - 8g_3^2 - \frac{9}{4}g_2^2 - \frac{17}{12}g_Y^2 - \frac{17}{12}g_{\text{mix}}^2 - \frac{2}{3}g_{B-L}^2 - \frac{5}{3}g_{B-L}g_{\text{mix}} \right) \\
& + \frac{y_t}{(4\pi)^4} \left\{ -12y_t^4 - \frac{27}{4}y_\nu^4 - \frac{27}{4}y_t^2y_\nu^2 - \frac{9}{4}Y_R^2y_\nu^2 + 6\lambda^2 + \frac{1}{2}\kappa^2 - 12\lambda y_t^2 \right. \\
& + y_t^2 \left(36g_3^2 + \frac{225}{16}g_2^2 + \frac{131}{16}g_Y^2 + 3g_{B-L}^2 + \frac{131}{16}g_{\text{mix}}^2 + \frac{25}{4}g_{\text{mix}}g_{B-L} \right) \\
& + y_\nu^2 \left(\frac{45}{8}g_2^2 + \frac{15}{8}g_Y^2 + 15g_{B-L}^2 + \frac{15}{8}g_{\text{mix}}^2 + \frac{15}{2}g_{\text{mix}}g_{B-L} \right) \\
& + \frac{502}{27}g_{\text{mix}}^3g_{B-L} + \frac{1085}{36}g_{\text{mix}}^2g_{B-L}^2 + \frac{502}{27}g_{\text{mix}}g_Y^2g_{B-L} + \frac{665}{27}g_{\text{mix}}g_{B-L}^3 + \frac{9}{4}g_2^2g_{\text{mix}}g_{B-L} \\
& - \frac{20}{9}g_3^2g_{\text{mix}}g_{B-L} + \frac{203}{27}g_{B-L}^4 + \frac{3}{4}g_2^2g_{B-L}^2 - \frac{8}{9}g_3^2g_{B-L}^2 + \frac{91}{12}g_Y^2g_{B-L}^2 + \frac{1187}{216}g_{\text{mix}}^4 - \frac{3}{4}g_2^2g_{\text{mix}}^2 \\
& \left. + \frac{19}{9}g_3^2g_{\text{mix}}^2 + \frac{1187}{108}g_{\text{mix}}^2g_Y^2 - \frac{23}{4}g_2^4 - 108g_3^4 + \frac{1187}{216}g_Y^4 + 9g_2^2g_3^2 - \frac{3}{4}g_2^2g_Y^2 + \frac{19}{9}g_3^2g_Y^2 \right\}, \tag{60}
\end{aligned}$$

$$\begin{aligned}
\frac{dy_\nu}{dt} = & \frac{y_\nu}{(4\pi)^2} \left(-3g_{\text{mix}}g_{B-L} - 6g_{B-L}^2 - \frac{3}{4}g_{\text{mix}}^2 - \frac{3}{4}g_Y^2 - \frac{9}{4}g_2^2 + \frac{1}{4}Y_R^2 + 3y_t^2 + \frac{9}{2}y_\nu^2 \right) \\
& + \frac{y_\nu}{(4\pi)^4} \left\{ -12y_\nu^4 - \frac{27}{4}y_t^4 - \frac{5}{4}Y_R^4 - y_\nu^2 \left(\frac{27}{4}y_t^2 + \frac{21}{8}Y_R^2 \right) + 6\lambda^2 + \frac{1}{2}\kappa^2 - 12\lambda y_\nu^2 - \kappa Y_R^2 \right. \\
& + y_\nu^2 \left(\frac{225}{16}g_2^2 + \frac{123}{16}g_Y^2 + 27g_{B-L}^2 + \frac{123}{16}g_{\text{mix}}^2 + \frac{69}{4}g_{\text{mix}}g_{B-L} \right) \\
& + y_t^2 \left(20g_3^2 + \frac{45}{8}g_2^2 + \frac{85}{24}g_Y^2 + \frac{5}{3}g_{B-L}^2 + \frac{85}{24}g_{\text{mix}}^2 + \frac{25}{6}g_{\text{mix}}g_{B-L} \right) + Y_R^2 (22g_{B-L}^2 + 3g_{\text{mix}}g_{B-L}) \\
& + 21g_{\text{mix}}^3g_{B-L} + \frac{799}{12}g_{\text{mix}}^2g_{B-L}^2 + 21g_{\text{mix}}g_Y^2g_{B-L} + \frac{253}{3}g_{\text{mix}}g_{B-L}^3 + \frac{9}{4}g_2^2g_{\text{mix}}g_{B-L} + 65g_{B-L}^4 \\
& \left. + \frac{27}{4}g_2^2g_{B-L}^2 + \frac{187}{12}g_Y^2g_{B-L}^2 + \frac{35}{24}g_{\text{mix}}^4 - \frac{9}{4}g_2^2g_{\text{mix}}^2 + \frac{35}{12}g_{\text{mix}}^2g_Y^2 - \frac{23}{4}g_2^4 + \frac{35}{24}g_Y^4 - \frac{9}{4}g_2^2g_Y^2 \right\}, \tag{61}
\end{aligned}$$

$$\begin{aligned}
\frac{dY_R}{dt} &= \frac{Y_R}{(4\pi)^2} \left(\frac{5}{2} Y_R^2 + 2y_\nu^2 - 6g_{B-L}^2 \right) \\
&+ \frac{Y_R}{(4\pi)^4} \left\{ -5Y_R^4 - \frac{19}{2} Y_R^2 y_\nu^2 - 9y_t^2 y_\nu^2 - \frac{27}{2} y_\nu^4 + 4\lambda_\Psi^2 + \kappa^2 - 8\kappa y_\nu^2 - 8\lambda_\Psi Y_R^2 \right. \\
&+ y_\nu^2 \left(\frac{51}{4} g_2^2 + \frac{17}{4} g_Y^2 + 16g_{B-L}^2 + \frac{17}{4} g_{\text{mix}}^2 + 11g_{\text{mix}} g_{B-L} \right) + \frac{103}{2} Y_R^2 g_{B-L}^2 \\
&\left. - 127g_{B-L}^4 - \frac{35}{6} g_{\text{mix}}^2 g_{B-L}^2 - \frac{32}{3} g_{\text{mix}} g_{B-L}^3 \right\}, \tag{62}
\end{aligned}$$

$$\begin{aligned}
\frac{d\lambda_\Psi}{dt} &= \frac{1}{(4\pi)^2} \left(\lambda_\Psi (20\lambda_\Psi - 48g_{B-L}^2 + 6Y_R^2) + 2\kappa^2 + 96g_{B-L}^4 - 3Y_R^4 \right) \\
&+ \frac{1}{(4\pi)^4} \left\{ -240\lambda_\Psi^3 - 20\kappa^2 \lambda_\Psi - 8\kappa^3 + \lambda_\Psi \left(\frac{1280}{3} g_{\text{mix}} g_{B-L}^3 + \frac{844}{3} g_{\text{mix}}^2 g_{B-L}^2 + 2112g_{B-L}^4 \right) \right. \\
&+ 448\lambda_\Psi^2 g_{B-L}^2 - 7168g_{B-L}^6 - \frac{8192}{3} g_{\text{mix}} g_{B-L}^5 - \frac{5344}{3} g_{\text{mix}}^2 g_{B-L}^4 + 12Y_R^4 g_{B-L}^2 + 288Y_R^2 g_{B-L}^4 \\
&+ 30\lambda_\Psi Y_R^2 g_{B-L}^2 - 60Y_R^2 \lambda_\Psi^2 + \lambda_\Psi (3Y_R^4 - 18Y_R^2 y_\nu^2) + 12Y_R^4 y_\nu^2 + 12Y_R^6 - 12\kappa^2 (y_t^2 + y_\nu^2) \\
&\left. + \kappa^2 (12g_2^2 + 4g_Y^2 + 4g_{\text{mix}}^2) + 40\kappa g_{\text{mix}}^2 g_{B-L}^2 \right\}, \tag{63}
\end{aligned}$$

$$\begin{aligned}
\frac{d\lambda}{dt} = & \frac{1}{16\pi^2} \left(\lambda (24\lambda - 9g_2^2 - 3g_{\text{mix}}^2 - 3g_Y^2 + 12y_t^2 + 12y_\nu^2) + \frac{3}{4} (g_Y^2 + g_{\text{mix}}^2) g_2^2 + \frac{3}{4} g_{\text{mix}}^2 g_Y^2 \right. \\
& \left. + \frac{9}{8} g_2^4 + \frac{3}{8} g_{\text{mix}}^4 + \frac{3}{8} g_Y^4 + \kappa^2 - 6y_t^4 - 6y_\nu^4 \right) \\
& + \frac{1}{(4\pi)^4} \left\{ -4\kappa^3 - 10\kappa^2\lambda - 312\lambda^3 + 36\lambda^2 (g_Y^2 + g_{\text{mix}}^2 + 3g_2^2) + \lambda \left(\frac{629}{24} g_Y^4 + \frac{629}{24} g_{\text{mix}}^4 + \frac{39}{4} g_{\text{mix}}^2 g_2^2 \right. \right. \\
& \left. \left. + \frac{39}{4} g_Y^2 g_2^2 - \frac{73}{8} g_2^4 + \frac{80}{3} g_{B-L} g_{\text{mix}}^3 + 34g_{B-L}^2 g_{\text{mix}}^2 + \frac{629}{12} g_{\text{mix}}^2 g_Y^2 + \frac{80}{3} g_{B-L} g_{\text{mix}} g_Y^2 \right) \right. \\
& \left. + \frac{305}{16} g_2^6 - \frac{289}{48} g_{\text{mix}}^2 g_2^4 - \frac{289}{48} g_Y^2 g_2^4 - \frac{559}{48} g_{\text{mix}}^4 g_2^2 - \frac{559}{48} g_Y^4 g_2^2 - \frac{32}{3} g_{B-L} g_{\text{mix}}^3 g_2^2 \right. \\
& \left. - 13g_{B-L}^2 g_{\text{mix}}^4 - \frac{379}{16} g_{\text{mix}}^2 g_Y^4 - \frac{32}{3} g_{B-L} g_{\text{mix}} g_Y^4 - \frac{32}{3} g_{B-L} g_{\text{mix}}^5 - 13g_{B-L}^2 g_{\text{mix}}^2 g_2^2 - \frac{559}{24} g_{\text{mix}}^2 g_Y^2 g_2^2 \right. \\
& \left. - \frac{379}{48} g_{\text{mix}}^6 - \frac{379}{48} g_Y^6 - \frac{32}{3} g_{B-L} g_{\text{mix}} g_Y^2 g_2^2 - \frac{379}{16} g_{\text{mix}}^4 g_Y^2 - \frac{64}{3} g_{B-L} g_{\text{mix}}^3 g_Y^2 - 13g_{B-L}^2 g_{\text{mix}}^2 g_Y^2 \right. \\
& \left. - y_t^4 \left(\frac{8}{3} g_Y^2 + 32g_3^2 + \frac{8}{3} g_{B-L}^2 + \frac{8}{3} g_{\text{mix}}^2 + \frac{20}{3} g_{B-L} g_{\text{mix}} \right) - y_\nu^4 (24g_{B-L}^2 + 12g_{B-L} g_{\text{mix}}) \right. \\
& \left. + y_t^2 \left(\frac{21}{2} g_{\text{mix}}^2 g_2^2 + \frac{21}{2} g_Y^2 g_2^2 + 6g_{B-L} g_{\text{mix}} g_2^2 - \frac{9}{4} g_2^4 - \frac{19}{4} g_{\text{mix}}^4 - \frac{19}{4} g_Y^4 - \frac{19}{2} g_{\text{mix}}^2 g_Y^2 - 4g_{B-L}^2 g_{\text{mix}}^2 \right. \right. \\
& \left. \left. - 10g_{B-L} g_{\text{mix}}^3 - 10g_{B-L} g_{\text{mix}} g_Y^2 \right) \right. \\
& \left. - y_\nu^2 \left(\frac{3}{2} g_{\text{mix}}^2 g_2^2 + \frac{3}{2} g_Y^2 g_2^2 + 18g_{B-L} g_{\text{mix}} g_2^2 + \frac{9}{4} g_2^4 + \frac{3}{4} g_{\text{mix}}^4 + \frac{3}{4} g_Y^4 + 18g_{B-L} g_{\text{mix}}^3 + 36g_{B-L}^2 g_{\text{mix}}^2 \right. \right. \\
& \left. \left. + \frac{3}{2} g_{\text{mix}}^2 g_Y^2 + 18g_{B-L} g_{\text{mix}} g_Y^2 \right) \right. \\
& \left. + \lambda y_t^2 \left(\frac{45}{2} g_2^2 + 80g_3^2 + \frac{85}{6} g_Y^2 + \frac{85}{6} g_{\text{mix}}^2 + \frac{20}{3} g_{B-L}^2 + \frac{50}{3} g_{B-L} g_{\text{mix}} \right) \right. \\
& \left. + \lambda y_\nu^2 \left(\frac{45}{2} g_2^2 + \frac{15}{2} g_Y^2 + 60g_{B-L}^2 + \frac{15}{2} g_{\text{mix}}^2 + 30g_{B-L} g_{\text{mix}} \right) \right. \\
& \left. - 144\lambda^2 (y_t^2 + y_\nu^2) - 3\lambda (y_t^4 + y_\nu^4 + 3y_\nu^2 Y_R^2) + 30y_t^6 + 30y_\nu^6 + 12y_\nu^4 Y_R^2 - 3\kappa^2 Y_R^2 \right. \\
& \left. + 32\kappa^2 g_{B-L}^2 + 20\kappa g_{B-L} g_{\text{mix}}^2 \right\}, \tag{64}
\end{aligned}$$

$$\begin{aligned}
\frac{d\kappa}{dt} = & \frac{1}{(4\pi)^2} \left\{ \kappa \left(4\kappa + 12\lambda + 8\lambda_\Psi - \frac{3}{2}g_y^2 - 24g_{B-L}^2 - \frac{3}{2}g_{\text{mix}}^2 - \frac{9}{2}g_2^2 + 3Y_R^2 + 6y_t^2 + 6y_\nu^2 \right) \right. \\
& \left. + 12g_{\text{mix}}^2g_{B-L}^2 - 12Y_R^2y_\nu^2 \right\} \\
& + \frac{1}{(4\pi)^4} \left\{ \kappa \left(-11\kappa^2 - 40\lambda_\Psi^2 - 48\kappa\lambda_\Psi - 60\lambda^2 - 72\kappa\lambda - (y_t^2 + y_\nu^2)(12\kappa + 72\lambda) - Y_R^2(6\kappa + 24\lambda_\Psi) \right. \right. \\
& - \frac{27}{2}y_t^4 - \frac{27}{2}y_\nu^4 - \frac{9}{2}Y_R^4 + \frac{21}{2}y_\nu^2Y_R^2 + g_2^2(3\kappa + 72\lambda) + g_Y^2(\kappa + 24\lambda) + g_{B-L}^2(16\kappa + 256\lambda_\Psi) \\
& + g_{\text{mix}}^2(\kappa + 24\lambda) + y_t^2 \left(\frac{45}{4}g_2^2 + 40g_3^2 + \frac{10}{3}g_{B-L}^2 + \frac{85}{12}g_{\text{mix}}^2 + \frac{85}{12}g_Y^2 + \frac{25}{3}g_{B-L}g_{\text{mix}} \right) \\
& + y_\nu^2 \left(\frac{45}{4}g_2^2 + 30g_{B-L}^2 + \frac{15}{4}g_{\text{mix}}^2 + \frac{15}{4}g_Y^2 + 15g_{B-L}g_{\text{mix}} \right) + 15Y_R^2g_{B-L}^2 \\
& - \frac{145}{16}g_2^4 + \frac{557}{48}g_Y^4 + 672g_{B-L}^4 + \frac{557}{48}g_{\text{mix}}^4 + \frac{15}{8}g_{\text{mix}}^2g_2^2 + \frac{15}{8}g_Y^2g_2^2 + \frac{40}{3}g_{B-L}g_{\text{mix}}^3 \\
& \left. + \frac{497}{3}g_{B-L}^2g_{\text{mix}}^2 + \frac{557}{24}g_{\text{mix}}^2g_Y^2 + \frac{40}{3}g_{B-L}g_{\text{mix}}g_Y^2 + \frac{640}{3}g_{B-L}^3g_{\text{mix}} \right) \\
& + y_\nu^2Y_R^2 \left(30Y_R^2 + 66y_\nu^2 - 84g_{B-L}^2 - \frac{3}{2}g_{\text{mix}}^2 - \frac{3}{2}g_Y^2 - 24g_{B-L}g_{\text{mix}} + \frac{9}{2}g_2^2 \right) \\
& - y_t^2(64g_{B-L}^4 + 76g_{B-L}^2g_{\text{mix}}^2 + 160g_{B-L}^3g_{\text{mix}}) - y_\nu^2(576g_{B-L}^4 + 12g_{B-L}^2g_{\text{mix}}^2 + 288g_{B-L}^3g_{\text{mix}}) \\
& - 18g_{B-L}^2g_{\text{mix}}^2Y_R^2 + 80\lambda_\Psi g_{B-L}^2g_{\text{mix}}^2 + 120\lambda g_{B-L}^2g_{\text{mix}}^2 \\
& - 45g_{B-L}^2g_{\text{mix}}^2g_2^2 - \frac{713}{3}g_{B-L}^2g_{\text{mix}}^4 - \frac{1024}{3}g_{B-L}^3g_{\text{mix}}^3 - 656g_{B-L}^4g_{\text{mix}}^2 - \frac{713}{3}g_{B-L}^2g_{\text{mix}}^2g_Y^2 \\
& \left. - \frac{512}{3}g_{B-L}^3g_{\text{mix}}^2g_Y^2 \right\}. \tag{65}
\end{aligned}$$

References

- [1] G. Aad *et al.* [ATLAS Collaboration], “Observation of a new particle in the search for the Standard Model Higgs boson with the ATLAS detector at the LHC,” Phys. Lett. B **716**, 1 (2012) [arXiv:1207.7214 [hep-ex]].
- [2] S. Chatrchyan *et al.* [CMS Collaboration], “Observation of a new boson at a mass of 125 GeV with the CMS experiment at the LHC,” Phys. Lett. B **716**, 30 (2012) [arXiv:1207.7235 [hep-ex]].

- [3] C. D. Froggatt and H. B. Nielsen, “Standard model criticality prediction: Top mass 173 ± 5 -GeV and Higgs mass 135 ± 9 -GeV,” *Phys. Lett. B* **368**, 96 (1996) [hep-ph/9511371].
- [4] C. D. Froggatt, H. B. Nielsen and Y. Takahashi, “Standard model Higgs boson mass from borderline metastability of the vacuum,” *Phys. Rev. D* **64**, 113014 (2001) [hep-ph/0104161].
- [5] H. B. Nielsen, “PREdicted the Higgs Mass,” arXiv:1212.5716 [hep-ph].
- [6] D. Buttazzo, G. Degrossi, P. P. Giardino, G. F. Giudice, F. Sala, A. Salvio and A. Strumia, “Investigating the near-criticality of the Higgs boson,” *JHEP* **1312**, 089 (2013) [arXiv:1307.3536 [hep-ph]].
- [7] M. Shaposhnikov and C. Wetterich, “Asymptotic safety of gravity and the Higgs boson mass,” *Phys. Lett. B* **683**, 196 (2010) [arXiv:0912.0208 [hep-th]].
- [8] K. A. Meissner and H. Nicolai, “Effective action, conformal anomaly and the issue of quadratic divergences,” *Phys. Lett. B* **660**, 260 (2008) [arXiv:0710.2840 [hep-th]].
- [9] V. V. Khoze, C. McCabe and G. Ro, “Higgs vacuum stability from the dark matter portal,” *JHEP* **1408**, 026 (2014) [arXiv:1403.4953 [hep-ph], arXiv:1403.4953].
- [10] H. Kawai and T. Okada, “Solving the Naturalness Problem by Baby Universes in the Lorentzian Multiverse,” *Prog. Theor. Phys.* **127**, 689 (2012) [arXiv:1110.2303 [hep-th]].
- [11] H. Kawai, “Low energy effective action of quantum gravity and the naturalness problem,” *Int. J. Mod. Phys. A* **28**, 1340001 (2013).
- [12] Y. Hamada, H. Kawai and K. Kawana, “Evidence of the Big Fix,” *Int. J. Mod. Phys. A* **29**, no. 17, 1450099 (2014) [arXiv:1405.1310 [hep-ph]].
- [13] Y. Hamada, H. Kawai and K. Kawana, “Weak Scale From the Maximum Entropy Principle,” arXiv:1409.6508 [hep-ph].
- [14] F. L. Bezrukov and M. Shaposhnikov, “The Standard Model Higgs boson as the inflaton,” *Phys. Lett. B* **659**, 703 (2008) [arXiv:0710.3755 [hep-th]].
- [15] Y. Hamada, H. Kawai and K. y. Oda, “Minimal Higgs inflation,” *PTEP* **2014**, 023B02 (2014) [arXiv:1308.6651 [hep-ph]].
- [16] Y. Hamada, H. Kawai, K. y. Oda and S. C. Park, “Higgs inflation still alive,” *Phys. Rev. Lett.* **112**, 241301 (2014) [arXiv:1403.5043 [hep-ph]].
- [17] Y. Hamada, H. Kawai, K. y. Oda and S. C. Park, “Higgs inflation from Standard Model criticality,” arXiv:1408.4864 [hep-ph].
- [18] Y. Hamada, K. y. Oda and F. Takahashi, “Topological Higgs inflation: The origin of the Standard Model criticality,” arXiv:1408.5556 [hep-ph].

- [19] Y. Kawamura, “Naturalness, Conformal Symmetry and Duality,” PTEP **2013**, no. 11, 113B04 (2013) [arXiv:1308.5069 [hep-ph]].
- [20] K. A. Meissner and H. Nicolai, “Conformal Symmetry and the Standard Model,” Phys. Lett. B **648**, 312 (2007) [hep-th/0612165].
- [21] N. Haba, H. Ishida, K. Kaneta and R. Takahashi, “Vanishing Higgs potential at the Planck scale in a singlet extension of the standard model,” Phys. Rev. D **90**, 036006 (2014) [arXiv:1406.0158 [hep-ph]].
- [22] Y. Hamada, H. Kawai and K. y. Oda, “Eternal Higgs inflation and cosmological constant problem,” arXiv:1501.04455 [hep-ph].
- [23] Y. Hamada, H. Kawai and K. y. Oda, “Predictions on mass of Higgs portal scalar dark matter from Higgs inflation and flat potential,” JHEP **1407**, 026 (2014) [arXiv:1404.6141 [hep-ph], arXiv:1404.6141].
- [24] K. Kawana, “The Multiple Point Principle of the Standard Model with Scalar Singlet Dark Matter and Right Handed Neutrinos,” arXiv:1411.2097 [hep-ph].
- [25] S. Iso, N. Okada and Y. Orikasa, “Classically conformal $B-L$ extended Standard Model,” Phys. Lett. B **676**, 81 (2009) [arXiv:0902.4050 [hep-ph]].
- [26] S. Iso and Y. Orikasa, “TeV Scale B-L model with a flat Higgs potential at the Planck scale - in view of the hierarchy problem -,” PTEP **2013**, 023B08 (2013) [arXiv:1210.2848 [hep-ph]].
- [27] N. Okada and O. Seto, “Higgs portal dark matter in the minimal gauged $U(1)_{B-L}$ model,” Phys. Rev. D **82**, 023507 (2010) [arXiv:1002.2525 [hep-ph]].
- [28] N. Okada, M. U. Rehman and Q. Shafi, “Non-Minimal B-L Inflation with Observable Gravity Waves,” Phys. Lett. B **701**, 520 (2011) [arXiv:1102.4747 [hep-ph]].
- [29] G. Aad *et al.* [ATLAS Collaboration], “Search for high-mass dilepton resonances in pp collisions at $\sqrt{s} = 8$ TeV with the ATLAS detector,” Phys. Rev. D **90**, no. 5, 052005 (2014) [arXiv:1405.4123 [hep-ex]].
- [30] P. H. Chankowski, S. Pokorski and J. Wagner, “Z-prime and the Appelquist-Carrazzone decoupling,” Eur. Phys. J. C **47**, 187 (2006) [hep-ph/0601097].
- [31] M. S. Carena, A. Daleo, B. A. Dobrescu and T. M. P. Tait, “ Z' gauge bosons at the Tevatron,” Phys. Rev. D **70**, 093009 (2004) [hep-ph/0408098].
- [32] P. A. R. Ade *et al.* [Planck Collaboration], “Planck 2015 results. XIII. Cosmological parameters,” arXiv:1502.01589 [astro-ph.CO].
- [33] P. A. R. Ade *et al.* [BICEP2 Collaboration], “Detection of B-Mode Polarization at Degree Angular Scales by BICEP2,” Phys. Rev. Lett. **112**, 241101 (2014) [arXiv:1403.3985 [astro-ph.CO]].

- [34] M. J. Mortonson and U. Seljak, “A joint analysis of Planck and BICEP2 B modes including dust polarization uncertainty,” JCAP **1410**, no. 10, 035 (2014) [arXiv:1405.5857 [astro-ph.CO]].
- [35] R. Flauger, J. C. Hill and D. N. Spergel, “Toward an Understanding of Foreground Emission in the BICEP2 Region,” JCAP **1408**, 039 (2014) [arXiv:1405.7351 [astro-ph.CO]].
- [36] N. Okada, V. N. Şenoğuz and Q. Shafi, “Simple Inflationary Models in Light of BICEP2: an Update,” arXiv:1403.6403 [hep-ph].
- [37] M. E. Machacek and M. T. Vaughn, “Two Loop Renormalization Group Equations in a General Quantum Field Theory. 1. Wave Function Renormalization,” Nucl. Phys. B **222**, 83 (1983).
- [38] M. E. Machacek and M. T. Vaughn, “Two Loop Renormalization Group Equations in a General Quantum Field Theory. 2. Yukawa Couplings,” Nucl. Phys. B **236**, 221 (1984).
- [39] M. E. Machacek and M. T. Vaughn, “Two Loop Renormalization Group Equations in a General Quantum Field Theory. 3. Scalar Quartic Couplings,” Nucl. Phys. B **249**, 70 (1985).
- [40] R. M. Fonseca, M. Malinský and F. Staub, “Renormalization group equations and matching in a general quantum field theory with kinetic mixing,” Phys. Lett. B **726**, 882 (2013) [arXiv:1308.1674 [hep-ph]].